NJC

ROYAL SOCIETY OF CHEMISTRY

PERSPECTIVE

View Article Online
View Journal | View Issue



Cite this: *New J. Chem.*, 2020, **44**, 3546

# Recent advances in organic dyes and fluorophores comprising a 1,2,3-triazole moiety

Damien Brunel * and Frédéric Dumur *

Received 21st December 2019,
Accepted 31st January 2020

DOI: 10.1039/c9nj06330g

rsc.li/njc

Since the discovery of the copper catalyzed azide alkyne cycloaddition in the early 2000s, tremendous efforts have been devoted to enlarging the scope of applications of this relatively simple to handle reaction. The chemistry of dyes has not been excluded from this enthusiasm so that a wide range of compounds have been synthesized over the years. Several key elements have sustained such research activity, such as the possibility to fine tune the photophysical properties, the easiness of structure screening in order to optimize the optical properties or the thermal stability of the triazole moiety. In this review, an overview of different dyes as well as their applications is reported.



## 1 Introduction

The independent discovery at the beginning of the 21st century of the copper-catalyzed version of the well-known azide–alkyne 1,3-dipolar cycloaddition by Medal and then Sharpless has enabled the introduction of the concept of click chemistry in modern chemistry.[1,2] This cycloaddition reaction, also known as the Huisgen reaction and reported for the first time by Huisgen in the 60s,[3] has revolutionized the way to create molecules by its simplicity and its efficacy. Indeed, click chemistry consists in mimicking Nature, which fabricates natural substances by joining together elemental building blocks by means of a simple and easy reaction. More generally, click chemistry is based on reactions where two specific functional groups react together in soft conditions *i.e.* in non-dangerous solvents and at room temperature, without formation of by-products and in high yields. Moreover, the structures of the potential substrates being limitless, an infinite diversity of structures can be formed. Benefiting from this versatility, click chemistry was notably used to produce numerous molecules with applications ranging from pharmaceuticals[4–6] to materials,[7,8] modified alkaloids,[9] carbohydrate chemistry,[10] crop protection products (antifungal or pesticides),[11,12] *etc.*[13,14] The azide alkyne cycloaddition involves a reaction between an azide and an alkyne, producing a stable 1,2,3-triazole ring. The thermal cycloaddition of an azide and an alkyne furnishes most of the time a mixture of two regioisomers: the 1,4-disubstituted triazoles and the 1,5-disubstituted triazoles. Selectivity between the two regioisomers can however be obtained by a careful selection of the metal catalyst. Thus, CuAAC (copper catalyzed azide alkyne cycloaddition) is a convenient way to produce specifically the 1,4-triazole ring whereas ruthenium-catalyzed azide–alkyne cycloaddition (RuAAC) only provides the 1,5-regioisomers (see Scheme 1).

If click chemistry has been extensively studied for the design of molecules with biological applications, use of click chemistry for the design of chromophores and photoluminescent molecules is more scarce, even if the triazole ring can be advantageously used to connect under mild conditions an electron-donating group to an electron accepting group.[15] Notably, the triazole ring offers a unique opportunity to give elaborate push–pull dyes which are now commonly used as photoinitiators of polymerization.[16–23] Consequently, this heterocyclic five-membered ring is mainly used as a π-conjugated spacer ensuring electronic communication between the electron-donating and accepting moieties. In this review, an overview of the different chromophores and photoluminescent push–pull molecules prepared by click chemistry is presented. Beyond the synthesis of these compounds, the different applications in which these different structures have been used are also presented.

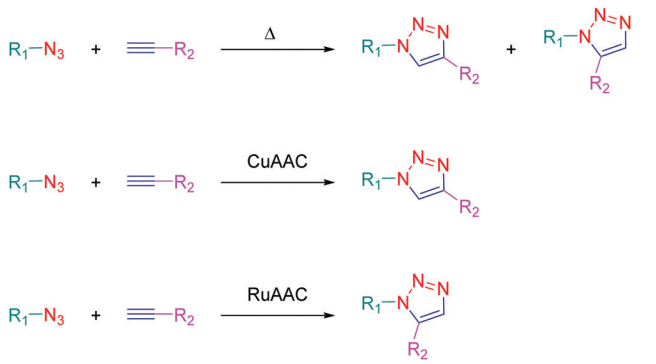


Scheme 1 The different types of cycloadditions based on the combination of an alkyne and an azide.

*Aix Marseille Univ, CNRS, ICR, UMR 7273, 13397 Marseille, France*

 

## 2. Push–pull molecules and light responsive organic molecules containing triazoles

The association of an electron donor and an electron acceptor connected by means of a triazole ring was done for the first time in 2005 by Blanchard-Desce and coworkers.[24,25] To examine the specificity introduced by the presence of the triazole ring in the push–pull dyes, a comparison was established between a series of dyes previously reported in the literature by the same authors and comprising alkene or alkyne spacers (*i.e.* compounds **1–3**) and the newly developed triazole-based dyes **4** and **5** (see Fig. 1).[26]

Starting from the commercially available tris(4-ethynylphenyl)-amine **6**, 4,4′-diethynylbiphenyl **7** and *N*-(4-azidophenyl)-*N*-hexanoyl-hexanamide **8**, the two products **4** and **5** could be formed in good yields, 68 and 86% respectively (see Scheme 2). The optical properties of the two dyes **4** and **5** were compared with those of their analogues **1–3** comprising π-conjugated spacers classically used for the design of push–pull dyes (see Table 1).[27] While comparing the absorption properties of the star-shaped dyes **1** and **4**, a hypsochromic shift of *ca.* 40 nm of the position of the intramolecular charge transfer (ICT) band could be observed for **4** compared to that of **1**. Similarly, a two-fold reduction of the photoluminescence quantum yield (PLQY) for **4** compared to that of **1** was also detected. A more severe reduction of the PLQY was demonstrated for **5**, the latter being divided by a factor 3.9 compared to that of its analogue **2**. While examining the order of the ICT bands, the most blue-shifted ICT band was found for **5** bearing the triazole ring, followed by

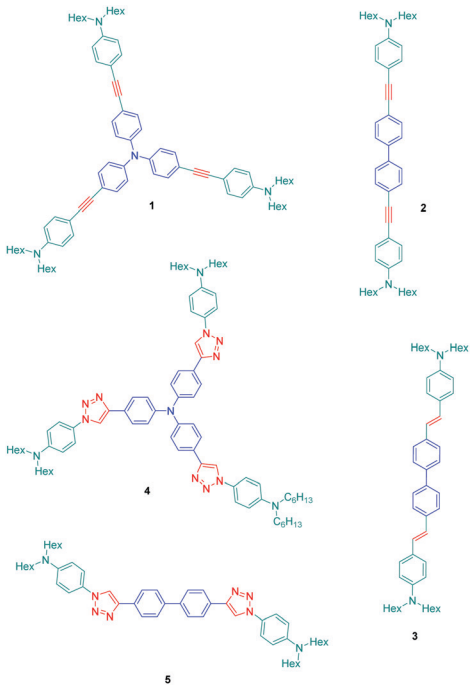

Fig. 1 Structures of triazole-based dyes **4** and **5** and their alkyne/alkene bridged analogues **1–3**.

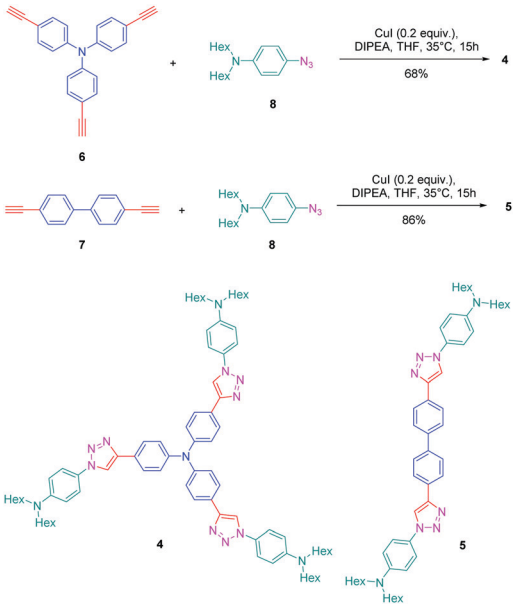


Scheme 2 Synthetic pathways to **4** and **5**.

Table 1 Photophysical characteristics of triazole-based dyes **1–5** in toluene

| Molecules | $\lambda_{abs}$ [a] (nm) | $\lambda_{em}$ [a] (nm) | $\Phi_F$ [b] | Stokes shift ($cm^{-1}$) | Ref. |
|---|---|---|---|---|---|
| **1** | 385 | 411 | 0.77 | 1634 | 6 |
| **4** | 347 | 387 | 0.49 | 3000 | 9 |
| **2** | 374 | 424 | 0.90 | 3200 | 9 |
| **3** | 401 | 456 | 0.84 | 3000 | 9 |
| **5** | 325 | 391 | 0.23 | 5100 | 6 |

[a] Recorded in toluene. [b] Photoluminescence quantum yield.

**2** and **3** bearing an alkene and an alkyne spacer respectively. Therefore, it can be concluded that the 1,2,3-triazole ring is the worse candidate to connect the electron donor to the electron acceptor, the blue-shift of the ICT band being indicative of a lack of electronic communication between the two partners.

If the detrimental effect of the 1,2,3-triazole ring on the electronic delocalization of **4** and **5** could be easily evidenced with a significant reduction of the PLQYs and a blue-shift of the ICT bands compared to those of **1–3**, conversely, the greatest Stokes shifts were determined for these dyes. Indeed, if Stokes shifts of 3200 and 3000 $cm^{-1}$ were found for **2** and **3** respectively, this value increased up to 5100 $cm^{-1}$ for the triazole-based dye **5**. Therefore, based on the large Stokes shifts, it can be concluded that a major electronic redistribution occurs prior to emission. Following this pioneering work, several derivatives still based on the triphenylamine electron donor were prepared and examined for their photophysical properties. In fact, triphenylamine is at the basis of numerous compounds developed for photovoltaic applications due to its remarkable charge transport ability and its low oxidation potential.[28–36] The chemical structures of the different triphenylamine-based dyes **9–11** synthesized by click chemistry are presented in Fig. 2.[37] To prepare **9–11**, mono, bis and tris-ethynyl-substituted triphenylamines **12–14** were engaged in reactions with 3-(4-azido-2,5-bis(hexyloxy)phenyl)-2-cyano-acrylic acid **15**

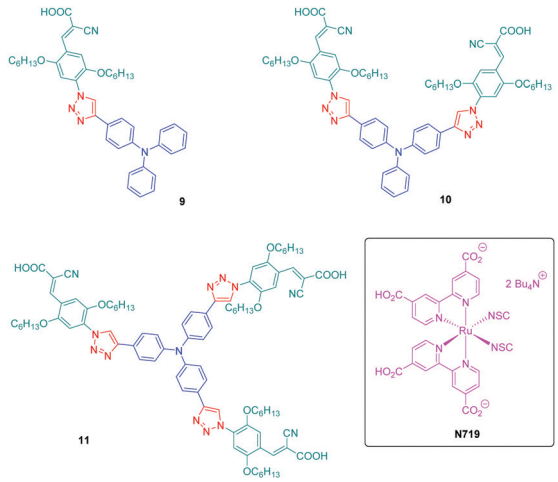


Fig. 2 The three triphenylamine-based dyes **9–11** and the reference dye **N719**.

in a THF–$H_2O$ mixture using sodium ascorbate and copper sulfate as the catalysts. **9–11** could be prepared with reaction yields ranging from 77 to 87%. 3-(4-Azido-2,5-bis(hexyloxy)phenyl)-2-cyanoacrylic acid **15**, which constitutes the precursor of the electron accepting part of the push–pull dyes **9–11**, is substituted with a cyanoacetic acid moiety favourable for the adsorption of the dye onto the $TiO_2$ electrode. This intermediate could be prepared in a 4-step procedure depicted in Scheme 3.[33,38]

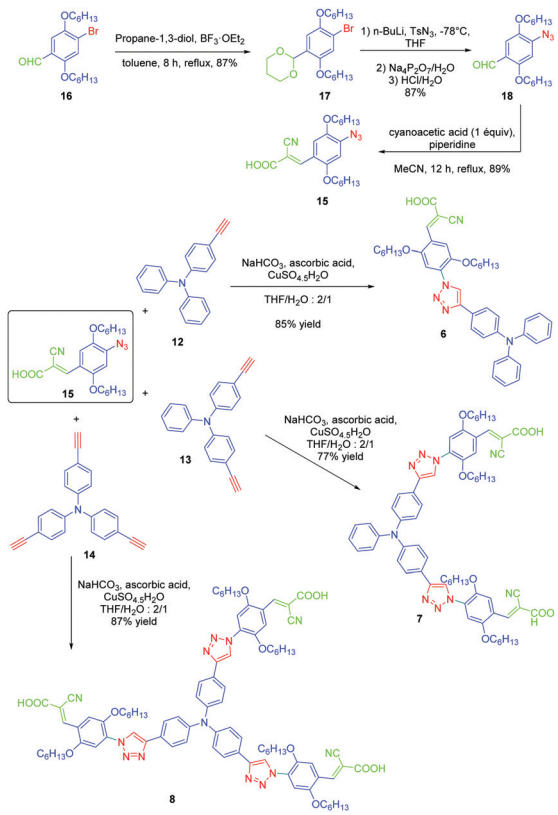


Scheme 3 Synthetic routes to 3-(4-azido-2,5-bis(hexyloxy)phenyl)-2-cyanoacrylic acid **15** later used for the synthesis of **9–11**.

Notably, after protection of the aldehyde group of **16** with propane-1,3-diol, acetal **17** could be formed in 87% yield. Finally, the azido group could be introduced in 87% yield using *n*-butyl lithium as the base. After deprotection of the aldehyde, a Knoevenagel reaction carried out on **18** with cyanoacetic acid provided the targeted intermediate **15** in 89% yield.

**9–11** were analysed by UV-visible absorption spectroscopy and cyclic voltammetry, and finally characterized as potential candidates for dye sensitized solar cells (DSSCs). The efficiencies of the corresponding solar cells remained moderate, the photon-to-electron conversion efficiency peaking at 3.00% for **9** (see Table 2). Interestingly, a reduction of the energy conversion efficiency was found while increasing the number of branches on the triphenylamine moiety, which was attributed to a reduced density of molecules on the $TiO_2$ anode. Indeed, by increasing the number of branches, a dramatic increase of the molecule size occurs requiring more space to be attached on the electrode, thus lowering the photon-to-electron conversion. All dyes showed a broad absorption band in the solid state ranging between 300 nm and 500 nm with a long tail extending until 700 nm. More precisely, for **9** and **10**, the absorption spectra showed two peaks, one around 310 nm attributable to π–π* transitions and a second one at 400 nm corresponding to the ICT band. Conversely, for **11**, a strong overlap of the π–π* transitions and the ICT band was found so that the absorption band at high energy was detected as a simple shoulder of the ICT band. The bathochromic shift of the ICT bands from **11** to **9** can be explained by a higher polarity of the molecule upon reduction of the branch number, facilitating the delocalization of electrons upon photoexcitation.

Theoretical calculations revealed the HOMO and LUMO energy levels of **9–11** to be spatially well-separated thanks to the presence of the triazole group. Indeed, the HOMO level was determined as being centered on the triphenylamine moiety whereas the LUMO level was localized on the anchoring group (*i.e.* the cyanoacetic acid group). Due to this well-defined separation between the HOMO and LUMO energy levels, efficient injection of the electrons into the conduction band of $TiO_2$ is expected upon photoexcitation. Cyclic voltammetry showed the dyes to be good candidates for photovoltaic applications due to their energy levels perfectly fitting with those of the adjacent layers. Notably, the position of the LUMO level at −3.50 eV is favourable for electron injection into the conduction band of $TiO_2$.

Table 2 Properties of the triphenylamine-based dyes **9–11**

| Dye | $\lambda_{max}$[a] (nm) | $\varepsilon$[b] ($10^4$ $M^{-1}$ $cm^{-1}$) | $E_{red}$ (V)/ LUMO[c] (eV) | $E_{ox}$ (V)/ HOMO[d] (eV) | $\eta$ (%) |
|---|---|---|---|---|---|
| **9** | 312, 388 | 3.28, 1.51 | −0.86/−3.50 | 0.96/−5.32 | 3.00 |
| **10** | 320, 405 | 6.00, 3.73 | −0.83/−3.54 | 0.91/−5.28 | 2.13 |
| **11** | 348 | 6.08 | −0.81/−3.51 | 0.98/−5.3 | 1.58 |
| **N719** | — | — | — | — | 4.86 |

[a] In dioxane with $C = 1 \times 10^{-5}$ M. [b] Molar extinction coefficient at $\lambda_{max}$ in solution. [c] Estimated from the onset reduction potential/calculated with the formula $E_{LUMO}$ (eV) = $-(E_{red} + [4.8 - E_{(Fc/Fc^+)}])$ eV. [d] Estimated from the onset oxidation potential/calculated with the formula $E_{HOMO}$ (eV) = $-(E_{ox} + [4.8 - E_{(Fc/Fc^+)}])$.

 

Similarly, the position of the HOMO level at −5.30 eV is lower than that of the $I^-/I_3^-$ redox potential so that the different dyes can be efficiently regenerated during device operation.[39,40] Parallel to the molecular size, which increases with the number of branches on the triphenylamine core, the low energy conversion efficiency could also be assigned to the limited absorption ability of triazole-linked push–pull dyes **9–11**, only partially covering the solar spectrum. On the contrary, the reference device fabricated with **N719** could provide a higher conversion efficiency by overcoming this drawback (see Table 2). Notably, **N719** exhibits two main absorption bands at 380 and 550 nm so that its absorption spectrum almost extends from 350 until 800 nm.

To establish a clear structure–performance relationship, the synthesis of numerous derivatives is a prerequisite. This hard work was notably done with a series of twelve dyes (**19–30**) prepared by click chemistry and comprising a 1,2,3-triazole ring. In this context, guidelines concerning the introduction of 1,2,3-triazole rings in push–pull dyes could be established. The photophysical properties of these dyes were compared to an analogue series (**31–33**) composed of 3 dyes bearing a phenyl spacer instead of the triazole ring.[41] In fact, to clearly evidence the real impact of the triazole ring on the photophysical properties, two series of triazole-based dyes were prepared, the first one (**19–27**) bearing the five-membered ring in an inverted position compared to the second one (**28–30**), generating two groups of regioisomers (see Scheme 4 and Fig. 3).

From a synthetic point of view, the first series (**19–27**) was prepared while using the azide group attached to the electron-donating moiety (**34–36**). The click reaction carried out under microwave irradiation could provide the different dyes with reaction yields ranging from 54 to 91% upon irradiating the solutions for 30–60 minutes. On the contrary, for the inverted series, the synthetic procedure should be modified for the preparation of **29** and **30**, 2-azidopyridine and 2-azidopyrimidine being less reactive than azidobenzene due to the formation of the tetrazole ring by tautomeric equilibrium. In this context,

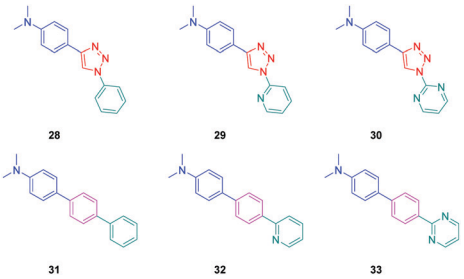


Fig. 3 Second series of push–pull molecules **28–33**.

classical thermal conditions were used. By refluxing in toluene with traces of benzene and while using copper triflate as the catalyst, **29** and **30** could be prepared in 68% and 12% yield respectively (see Scheme 5). Noticeably, if traces of benzene in toluene seem to be required for the reaction to proceed, no justification for its presence was mentioned by the authors. Finally, the three reference compounds **31–33** were obtained by a Suzuki cross-coupling reaction of bromobenzene, bromopyridine, or bromopyrimidine with the corresponding boronic ester (see Scheme 5). **31**, **32** and **33** could be obtained with reaction yields ranging from 49 to 86%.

The photophysical properties of the three series (**19–27**, **28–30**, and **31–33**) were examined to explore the exact role of the triazole spacer in the intramolecular charge transfer process. It has to be noticed that prior to this work, a similar comparison was made from a theoretical point of view by Catan and coworkers of **25** and **28** and the conclusions are consistent with those found in this work.[42,43] A summary of the absorption properties is provided in Table 3. As first findings, the different dyes **19–27** showed no or only weak emission in dichloromethane. Precisely, no emission could be detected for all dyes comprising a benzene ring as the electron donor. While comparing the variation of the absorption maximum for the same electron acceptor, a red-shift of the absorption maximum with the electron-releasing ability of the

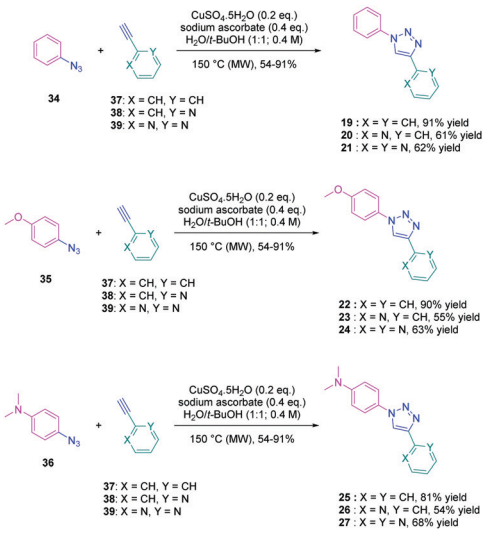


Scheme 4 Chemical structures and synthetic routes to **19–27**.

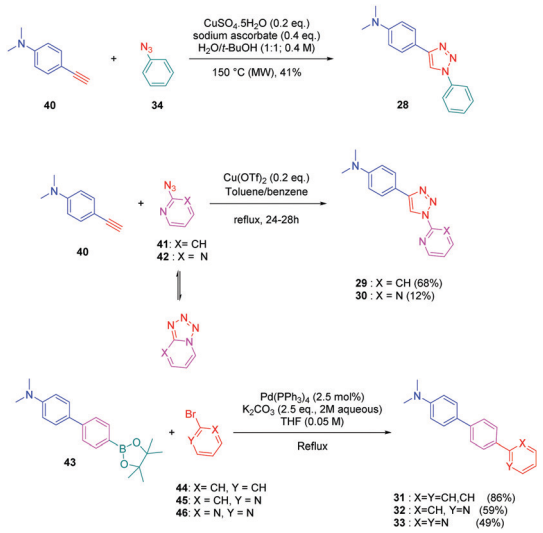


Scheme 5 Synthetic routes to **29–33**.

Table 3 UV-visible characteristics of push–pull molecules reported in ref. 27

| Dyes | $\lambda_{abs}$[a] (nm) | $\varepsilon$[a] ($M^{-1}$ $cm^{-1}$) | $\lambda_{em}$[a] (nm) | $k$[b] ($cm^{-1}$) |
|---|---|---|---|---|
| **19** | 250, 266 (sh), 272 (sh), 282 (sh), 289 (sh) | 23 140 | n.o.[c] | — |
| **20** | 286 | 23 140 | n.o.[c] | — |
| **21** | 255 | 4020 | n.o.[c] | — |
| **22** | 256, 267 (sh), 273 (sh) | 25 120 | n.o.[c] | — |
| **23** | 282 (sh), 289 (sh) | 25 600 | n.o.[c] | — |
| **24** | 287 | 27 180 | 392 | 6087 |
| **25** | 263 | 24 380 | n.o.[c] | — |
| **26** | 286 (sh), 302 | 20 940 | 396 | 12 729 |
| **27** | 306 | 23 920 | 413 | 22 048 |
| **28** | 309 | 20 020 | 454 | 27 609 |
| **29** | 270 (sh), 302 | 28 480 | 438 | 23 228 |
| **30** | 271 (sh), 296, 305 (sh), 345 (sh) | 27 660 | 470 | 26 593 |
| **31** | 268 (sh), 287, 310 (sh), 345 (sh) | 16 760 | n.o.[c] | — |
| **32** | 325 | 34 320 | 419 | 13 028 |
| **33** | 337 | 27 640 | 449 | 18 636 |

[a] Determined in dichloromethane with $C$ = 5 μM. [b] Slope of the linear correlation of the Stokes shift with the solvent orientation polarizability determined from the Lippert–Mataga plots. [c] Not observed.

donor was observed. Parallel to this, by improving the electron-withdrawing ability of the acceptor, a red-shift of the absorption maximum was similarly observed. While comparing with the reference series **31–33** comprising a benzene ring as the spacer, a larger red-shift of the absorption maximum with the donor strength was found ($\Delta\lambda_{max}$ = 26 nm) for this series (**31–33**) compared to the series (**19–27**) comprising the triazole group ($\Delta\lambda_{max}$ = 7 nm). This higher shift of the absorption maximum was assigned to a higher charge redistribution upon photoexcitation, evidencing better conjugation between the donor and the acceptor when a benzene ring is used as a spacer. The higher conjugation degree for the benzene-based series was also demonstrated while comparing the absorption maxima for **28** and **31**, respectively detected at 302 and 323 nm. Finally, the solvatochromism of the different dyes was rationalized using the Lippert–Mataga equation.[43] In all cases, a linear correlation was found, demonstrating the validity of the model. In this equation, the variation of the Stokes shift with the solvent polarity is examined, and the slope of the plots is directly related to the difference existing between the dipole moments in the ground and the excited state. Logically, for identical electron donors, a steeper slope was found while increasing the electron-accepting ability. But a deeper insight into the linear correlations unveiled more complex processes. Notably, comparison of the slopes for **28** and **31** revealed similar values, demonstrating that a similar charge redistribution occurs upon excitation. However, examination of the absorption and emission maxima of **28** and **31** also evidences the two maxima to be red-shifted for **31** compared to **28**, consistent with a higher conjugation degree for the dyes comprising a benzene spacer. Therefore, it was concluded from these different results that if better electronic conjugation exists in the ground state for the dyes (**31–33**) comprising a benzene spacer, higher charge transfer occurs for the triazole-based dyes (**19–27**) comprising a strong electron acceptor such as a pyridine or a pyrimidine moiety. Conversely, similar charge transfer is observed for the dyes comprising a weak electron acceptor such as benzene. Comparison of the regular series (**25**, **26** and **27**) with the inverted series (*i.e.* **28**, **29**, and **30**) revealed redshifted absorption for the inverted series. Comparison of the slopes of the Lippert–Mataga correlation of the regular and inverted series for dyes (**25–27** *vs.* **28–30**) comprising a strong electron acceptor also revealed the slopes for the inverted series (**28–30**) to be more pronounced than those of the regular series (**25–27**).

From these observations, it was concluded that for the inverted series, the triazole ring was acting as an electron acceptor. Overall, the orientation of the triazole ring in the regioisomers can efficiently influence the photophysical properties of the push–pull dyes. For most of the abovementioned dyes, crystals could be grown so that their Non-Linear Optical (NLO) response could be examined. However, as a prerequisite, only structures crystallizing in a non-centrosymmetric arrangement could be considered for their capabilities to produce a non-linear response. Among all dyes, only **22**, **23** and **24** were analyzed for their Second Harmonic Generation (SHG) efficiencies while using potassium dihydrogen phosphate (KDP) as a reference.

As predicted by the two-state model,[44] the best non-linear response was obtained for the dye exhibiting the strongest charge redistribution upon excitation and the non-linear response of **24** was 80 times higher than that of KDP. Conversely, the SHG efficiencies of **22** and **23** were 3.4 and 6 times higher than that of KDP. Prior to this work, numerous studies were carried out by the group of Fröhlich *et al.* on push–pull dyes comprising the 1,2,3-triazole ring as an electron-acceptor. In this field, the first report was published in 2011 with **47** crystallizing in the space group $P2_12_12_1$. This compound could be prepared in two steps, by thiophene-ring fragmentation (TRF) of (3-bromo-5-methylthiophen-2-yl)trimethylsilane.[45–47] Following the formation of the intermediate enyne, the click reaction of azidobenzene with the enyne derivative could provide the expected dye as the unique 1,4-regioisomer in 75% yield by using microwave irradiation (see Scheme 6).

Conversely, all attempts of synthesis using thermal conditions could only furnish **47** in 58% yield after 18 hours of heating at 50 °C. Importantly, the *Z*-geometry of **47** was of crucial importance to produce none-centrosymmetric crystals. Examination of the SHG response while exciting at 1064 nm revealed the NLO response to be two times higher than that of KDP.

Considering that the 1,2,3-triazole group acts as an electron acceptor in these structures, **47** was revisited in a more extended study (**47** and **51–59**) in which ten different groups were attached onto the five-membered ring (see Fig. 4).[48]

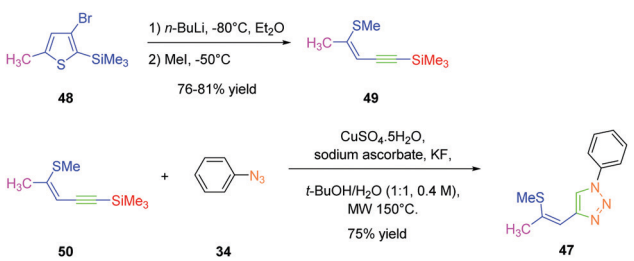


Scheme 6 Synthetic route to the push–pull dye **47**.

 

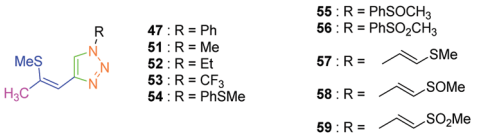


Fig. 4 Chemical structures of **47** and **51–59**.

While examining the substituent effects, substitution of the 1,2,3-triazole ring with aromatic rings (**54–56**) was determined as being preferable over vinylic (**57–59**) or aliphatic groups (**51–53**). Finally, for aromatic rings, the methylsulfone group (**55**) proved to be the best substituent for maximizing the hyperpolarizability tensors. Compared to **47** comprising an unsubstituted aromatic ring, an enhancement of the NLO response by a factor 3.5 was obtained for **56** substituted with a sulfone moiety (see Table 4).

Click chemistry being a versatile technique enabling one to perfectly control the regioselectivity, a comparison between 1,2 and 1,4-regioisomers was established.[49] Different groups were introduced onto the electron-donating thiol moiety, namely, methyl, ethyl, propyl and butyl groups. The different alkynes **50** and **60–64** were obtained by ring-opening of the thiophene derivatives **48**, **65**, and **66**. By applying a copper-catalysed click reaction to **50** and **60–64**, six different dyes **47** and **67–71** could be prepared with reaction yields ranging from 61 to 75%. Reflux in the presence of a catalytic amount of acid (HCl) could partially isomerize the *Z*-isomers **47**, **68**, **70** and **71** into the *E*-isomers **72**, **73**, **74** and **75** respectively in moderate yields (see Scheme 7). Indeed, for all dyes **47** and **67–75**, preparative thin layer chromatography (TLC) was required to separate the two isomers, providing in turn the *E*-isomers only in low yields. On the contrary, the ruthenium-catalyzed click reaction selectively furnished the 1,2-regioisomer. In this last case, only one derivative was prepared, namely **77** in 39% yield, starting from **76** formed by deprotection of the silyl group of **50**. Examination of the crystal structures of the different dyes revealed **70**, **71**, **72** and **77** to be unsuitable for NLO measurements due to centrosymmetric crystallization. Finally, the SHG signal detected for the 4-series was relatively low for two dyes *i.e.* **47** and **68** and no signals were detected for the others.

Isomerization of the double bond only provided the **72–74**-series crystallizing in a centrosymmetric arrangement. Modification of the substitution on the 1,2,3-triazole ring did not significantly modify the NLO response of **77**, approaching that of its 1,4-regioisomer **47**. Upon oxidation of the sulphur atom (**78** and **79**), the opposite situation to that found for the previous series could be created. Oxidation of sulphur to sulfone converted the electron-donating

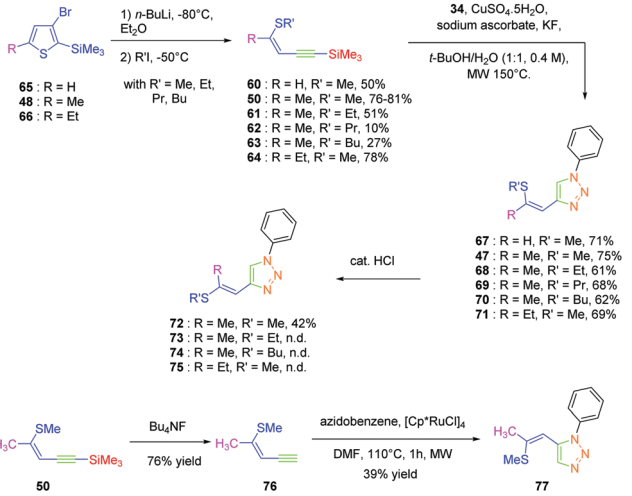


Scheme 7 Synthetic route to **47**, **67–71** and **77**.

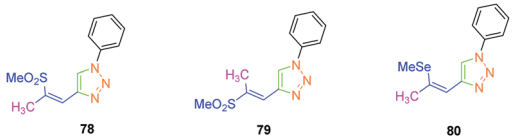


Fig. 5 Chemical structures of **78–80**.

group (sulphur) to the electron-accepting group (sulfone), inverting the push–pull effect. Two stereoisomers were prepared, namely **78** and **79** differing in the configuration of the double bond. While comparing **74** with its parent **47**, an enhancement of the NLO response by about 45% was found. Finally, the best results were obtained with the selenium-based analogue of **47** *i.e.* **80** (see Fig. 5). In this last case, the NLO response was enhanced by a factor of 20, resulting from the increased electron density in the π-conjugated system.

In 2017, the highest SHG efficiency ever reported for this family of dyes was reported by the same authors.[50] Interestingly, a great deal of effort was devoted to improving the synthetic route to these dyes with regards to the safety, the selectivity and the quantity of materials available at each step. By substituting **81**, **54** and **82** with methoxy, thiomethoxy and dimethylamino groups, D–A–D triads could be obtained (see Fig. 6). If **54** and **82** were determined as crystallizing in centrosymmetric arrangements, **81** crystallized in the $P2_{1/C}$ space group and showed an SHG response 80 times higher than the reference KDP.

In the previous studies of Fröhlich, substituents positioned on the 1,2,3-triazole ring were demonstrated to have no influence on

Table 4 Hyperpolarisability tensors in atomic units (a.u.) for the dyes **47** and **51–59**

| Dyes | **47** | **51** | **52** | **53** | **54** | **55** | **56** | **57** |
|---|---|---|---|---|---|---|---|---|
| $\beta_{tot}$ | 0.37 | 0.41 | 0.51 | 1.72 | 2.39 | 2.69 | 4.44 | 2.48 |
| Dyes | | | | **58** | | | | **59** |
| $\beta_{tot}$ | | | | 2.52 | | | | 3.19 |

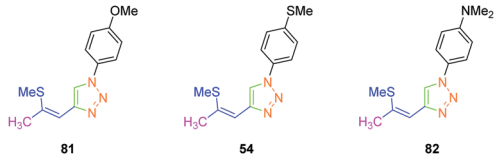


Fig. 6 Chemical structures of **54**, **81** and **82**.

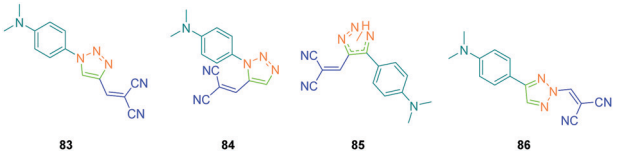


Fig. 7 The four positional isomers of dicyanovinyl-triazole-dimethylaminobenzene compounds **83–86**.

the SHG response, as quite similar responses were obtained with 1,2- and 1,4-regioisomers. This parameter was earlier studied by Diederich *et al.* and opposite conclusions were then established with **83–86** (see Fig. 7).[51] For this study, if potentially seven constitutional isomers could be prepared differing in the position of the electron-donating and electron-accepting groups around the triazole group, only four of them **83–86** were obtained.

From a synthetic point of view, the design of these four dyes proved to be a challenge. As shown in Scheme 8, **83** could only be obtained using a two-step procedure, by first performing the click reaction with propynal **87** and 4-azido-*N*,*N*-dimethylaniline **36** and by subsequently realizing the Knoevenagel reaction of **88**. Conversely, attempts of the click reaction with 4-azido-*N*,*N*-dimethylaniline **36** and 2-(3-(trimethylsilyl)prop-2-yn-1-ylidene)-malononitrile **89** only furnished **83** in low reaction yields (>5%). The reaction of 2-(3-(trimethylsilyl)prop-2-yn-1-ylidene) malononitrile **89** and 4-azido-*N*,*N*-dimethylaniline **36** was more efficient to prepare the 1,2-regioisomer **90**. In this last case, click chemistry was not the reaction used to prepare **90** but a thermal 1,3-dipolar cycloaddition. After 5 days of reflux, the intermediate silylated derivatives could be obtained in 18% yield and desilylation of **91** with methanol furnished **90** in 78% yield (see Scheme 9). If the reaction was low-yielding, the formation of **90** was highly selective, resulting from the bulkiness of the trimethylsilyl group.

Concerning **85** and **86**, the two molecules were synthesized by alternative synthetic routes to click chemistry or the thermal

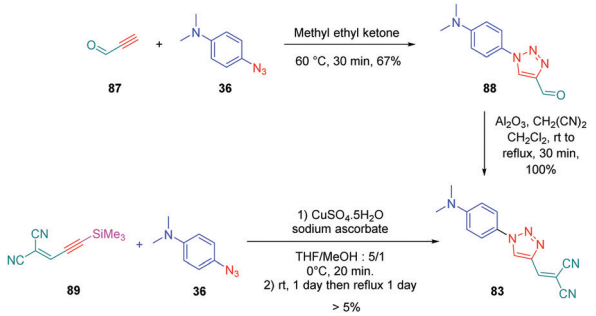


Scheme 8 Synthetic pathway of **83**.

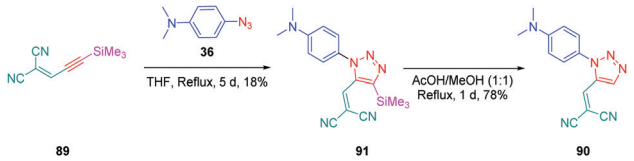


Scheme 9 The two-step synthetic route to **90**.

Huisgen reaction, these two procedures being unable to provide the two expected products. Thus, to prepare **85**, a simple cycloaddition reaction of 2-(3-(4-(dimethylamino)phenyl)prop-2-yn-1-ylidene)-malononitrile **92** with sodium azide upon heating at 100 °C formed **85** in 61% yield.

Conversely, **86** was obtained in more steps, the first one consisting of the click reaction between azidomethyl pivalate **93** and 4-ethynyl-*N*,*N*-dimethylaniline **94**, furnishing after basic treatment **73** in 51% yield. By an addition/elimination reaction of *N*,*N*-dimethyl-4-(2*H*-1,2,3-triazol-4-yl)aniline **95** with (chloromethylidene) propanedinitrile **96** carried out at room temperature, **86** could be obtained in 63% yield (see Scheme 10).

To examine the effect of the 1,2,3-triazole ring on the electronic delocalization between the electron-donating dimethylaminophenyl group and the electron accepting dicyanomethylidene group, a comparison of the photophysical properties of **83–86** was established with those of **97**[52] and **98**[53] previously reported in the literature. Precisely, the nature of the spacer and the number of carbon atoms between the donor and the acceptor were determined in previous work of the same group as being determinants of the photophysical properties of the dyes. In this context, **97** and **98** were selected for the comparison due to the similarity in the length of their π-conjugated spacers (see Fig. 8 and Table 5).[54]

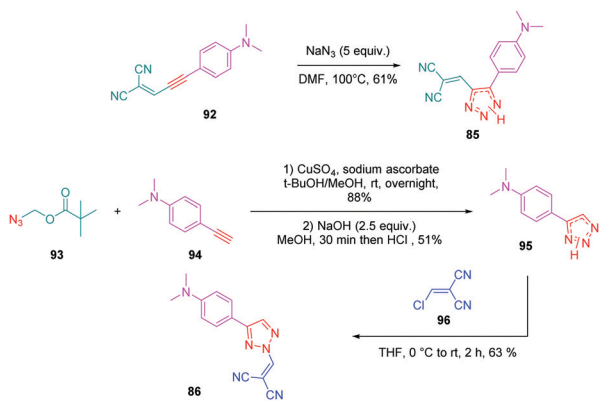


Scheme 10 Synthetic routes to **85** and **86**.

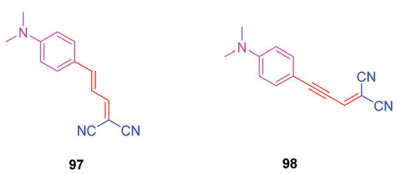


Fig. 8 Chemical structures of **97** and **98**.

 

Table 5 Optical properties of **83–86**, **97** and **98**

| Dyes | $\lambda_{abs}$ (nm) | $\varepsilon$ ($M^{-1}$ $cm^{-1}$) | Ref. |
|---|---|---|---|
| **83** | 400 | 8100 | 40 |
| **84** | 433 | 2500 | 40 |
| **85** | 423 | 11 300 | 40 |
| **86** | 453 | 7300 | 40 |
| **97** | 477 | 44 100 | 40 |
| **98** | 488 | 47 000 | 42 |

All spectra were recorded in $CH_2Cl_2$ at 298 K.

As the first finding, a clear reduction of the conjugation upon incorporation of the 1,2,3-triazole ring was determined for **83–86** relative to **97** and **98**. A blue-shift as high as 88 nm was measured between the absorption maxima of **83** and **98**. While examining the influence of the substitution pattern on the 1,2,3-triazole ring, the worst results were obtained upon substitution of nitrogen 1 of the triazole, clearly interrupting the conjugation in **83** and **84**. Conversely, upon substitution of nitrogen 2 of the triazole with an electron accepting group, an absorption maximum at 453 nm was found for **86**, shifted by 53 nm compared to **83** (see Table 5).

The well-established *N,N*-dimethylaminophenyl group was not the only electron donor to be used for the design of triazole-based push–pull dyes. Another electron-donating group of interest which is extensively used for the design of photoluminescent dyes was also employed, namely fluorene. Small molecules but also polymers[55] were prepared for their photoluminescence properties. Concerning small molecules, a series of four derivatives **99–101** varying in the substituent attached onto the electron accepting moiety was examined for their absorption and emission properties.[56] Using the standard conditions of click chemistry, the four compounds were obtained with reaction yields ranging from 72% for **99** to 79% for **100** and **101** by making a reaction between **103** with **34**, **35** with **104** or **34** with **105** (see Scheme 11). Surprisingly, examination of the absorption properties revealed the absorption maximum for **102** to be blue-shifted compared to **99–101** (295 nm *vs.* 300 nm), whereas **102** is substituted by the most electron-withdrawing group (see Table 6).

This blue-shift is the opposite situation to what is classically observed upon introduction of a nitro group onto a push–pull chromophore.[57,58] The authors tentatively assigned this unexpected shift to a reduction of the conjugation length, the electron-accepting group extending from the triazole ring to the aromatic ring. This trend was confirmed by photoluminescence, **102** again exhibiting the most blue-shifted emission (334 nm *vs.* 353 nm for **99**) (see Table 6). However, **102** was the most emissive compound of the series, its photoluminescence quantum yield peaking at 0.2%.

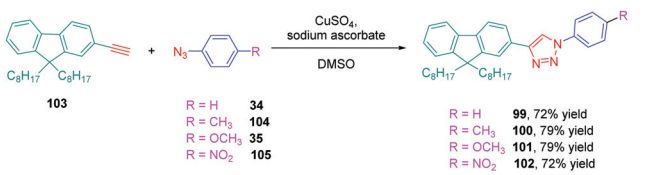


Scheme 11 Click chemistry reaction of four fluorene-triazole-pull molecules **99–102**.

Table 6 Physical properties of the four fluorene derivatives **106–113** reported in ref. 56

| Compounds | $\lambda_{abs}$ [a] (nm) | $\lambda_{em}$ [b] (nm) | $\Delta\lambda$ Stokes's (nm) | $\varepsilon$ ($M^{-1}$ $cm^{-1}$) |
|---|---|---|---|---|
| **99** | 300 | 353 | 53 | 8100 |
| **100** | 300 | 337 | 37 | 2500 |
| **101** | 300 | 339 | 39 | 11 300 |
| **102** | 295 | 334 | 39 | 7300 |

[a] Recorded in THF with $c$ = 10 μM at room temperature. [b] Upon excitation at 297 nm.

The solvatochromism of **99–102** in eight solvents revealed the four dyes to be insensitive to the solvent polarity while examining their absorption characteristics. The opposite situation was found for their emission properties. If the emission of **102** was also insensitive to the solvent polarity, broadening of the absorption spectra was found for **100** and **101** whereas a clear red shift from 342 nm in toluene to 363 nm in acetonitrile was found for **99** upon increasing the solvent polarity. To support the strong shift observed for **99**, the presence of excited state intramolecular charge transfer (ESICT) was proposed by the authors. This hypothesis was confirmed while using the Lippert–Mataga model. On the contrary, for **100** and **101**, an admixture of locally excited (LE) emission and intramolecular charge transfer emission was proposed to explain the near insensitivity of the emission to the solvent polarity.

Determination of the origin of the photoluminescence properties was performed with another series of dyes **106–113** based on polyaromatic structures.[59] As the main interest of this study, the authors succeeded in converting non-fluorescent or low emissive compounds into highly emissive dyes by simply realizing a click reaction (see Scheme 12). By making a reaction between 4-ethynyl-*N,N*-dimethylaniline **94** and 4-ethynylbenzonitrile **114** with four different aryl azides **35**, **105**, **115** and **116**, eight dyes **106–113** could be obtained with reaction yields ranging from 50 to 67%. As observed for the previous series of dyes, solvatochromism revealed

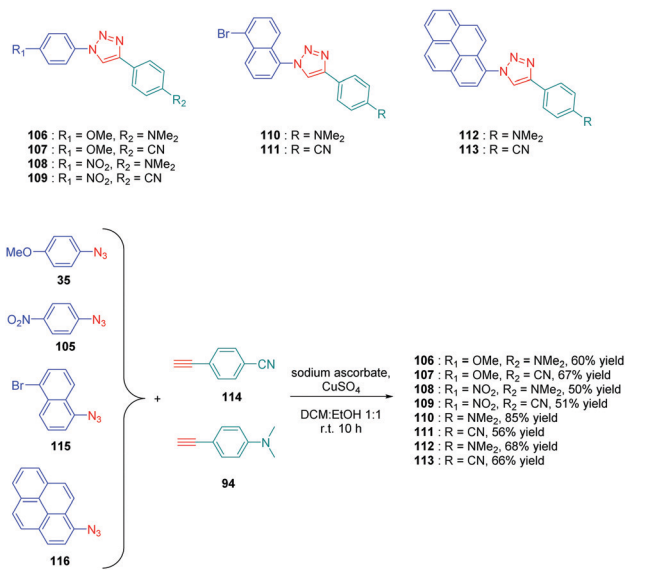


Scheme 12 Chemical structures of **106–113**.

the absorption maxima for all dyes to be not affected by the solvent polarity contrarily to the photoluminescence maxima. Concerning photoluminescence, an increase of the PLQY with the solvent polarity was demonstrated, evidencing a highly polar excited state. The lack of influence of the solvent polarity on the absorption properties was also indicative of intramolecular charge transfer originating from the lowest-lying excited state. The shift of the emission maximum proved to be relatively important, as exemplified with **106**, which showed a shift as high as 122 nm between hexane and methanol. Comparatively, **111** showed lower sensitivity, the shift being limited to 23 nm. Among the series of dyes, **112**, which comprises a pyrene moiety, proved to be the most interesting compound from the point of view of its emission. If a structureless emission peak was found in apolar solvents (cyclohexane and hexane), dual emission could be detected in polar solvents, one of the two peaks being characteristic of the emission of pyrene. In fact, coexistence of ICT emission and LE emission was determined in the PL spectra. Examination of the solvatochromic behaviour by using the Lippert–Mataga model confirmed the previous conclusions. Notably, the different linear correlations revealed the ground state of these dyes to be moderately polar and the emissive state to be highly polar, corresponding to ICT emission. Due to the unique ability of **112** to exhibit dual emission in polar solvents, this compound constitutes thus an excellent candidate for polarity sensing.

Over the years, a wide range of 1,2,3-triazole-based fluorogenic dyes **117–123** have been developed, especially for biolabeling applications as exemplified with the series of compounds presented in Fig. 9.[60–65] Indeed, *in vivo* bioimaging and theranostics are two active research fields requiring the rapid development of new structures.[66–72] In 2009, an extensive study was notably carried out on 102 dyes by making a reaction between 17 azides and 5 different xanthone or xanthene-based fluorophores.[73] However, conclusions were difficult to establish, no clear trend being detected. Concerning fluorenes, another series of dyes (**124–131**) was reported in 2013, incorporating diazines as electron acceptors.[74]

In this study, which required hard work for the synthesis with regards to the diversity of structures and the number

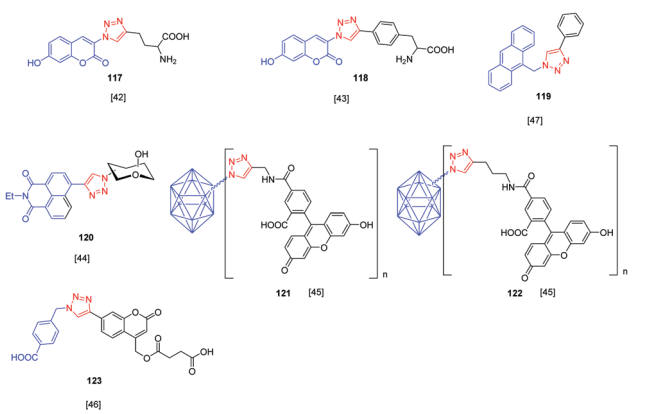


Fig. 9 Series of triazole-based dyes **117–123** used for biolabeling applications.

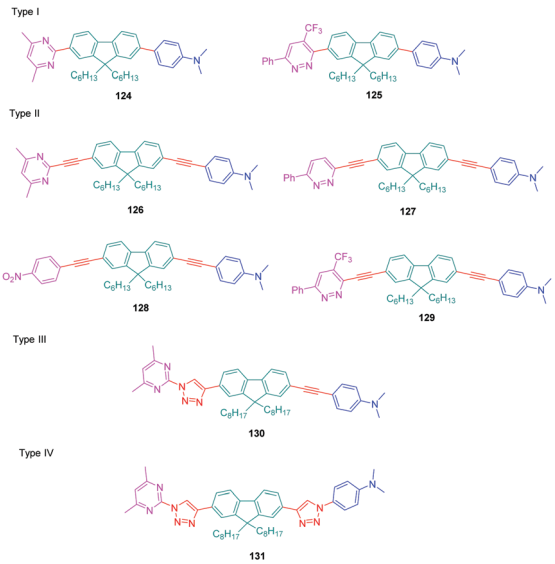


Fig. 10 Structures of the fluorene-based dyes **124–131** comprising a diazine (pyrimidine or pyridazine) as the electron accepting group.

of compounds, four series (I–IV) of D–π–A diads were elaborated, comprising the fluorene unit as a spacer connecting the electron-accepting diazine to the electron-donating *N,N*-dimethylaminobenzene, and differing in the length of the π-conjugated spacer. The structures of the four series of dyes are presented in Fig. 10, comprising as diazine groups pyridazines[75] or pyrimidines.[76]

In turn, numerous combinations based on different linkages (two triazoles, one triazole and one ethynyl bridge, two ethynyl groups, and two σ-bonds) could be prepared. A reference compound with a nitro end-group was also prepared for comparison. To create asymmetric structures, 2-bromo-9,9-dihexyl-7-iodo-9*H*-fluorene **132** proved to be the key element for these different syntheses. Starting from this intermediate, a double Sonogashira cross-coupling reaction with trimethylsilyl-acetylene **133** and triisopropylacetylene **135** enabled the introduction of two ethynyl groups end-capped with protecting groups that could be cleaved selectively with different reaction conditions. Using this strategy, **131** could be obtained after 6 steps in moderate yield (see Scheme 13). A more versatile synthetic route was developed for **105–108** and **109** since a common intermediate could be prepared in three steps starting from 2-bromo-9,9-dihexyl-7-iodo-9*H*-fluorene **111**. Finally, a Sonogashira coupling with the appropriate aryl halide could provide **105–108** with reaction yields ranging from 76 to 86% (see Scheme 14). Concerning **109**, reaction of the common intermediate with azidopyrimidine following a CuAAC procedure could provide **109** in 53% yield.

A similar approach was developed for the synthesis of **144** and **145** based on a Suzuki cross-coupling reaction this time (see Scheme 15). Despite the presence of two different halogens on 2-bromo-9,9-dihexyl-7-iodo-9*H*-fluorene **132**, the higher reactivity of the iodine atom over the bromine one was not totally respected, 20% of 4,4′-(9,9-dihexyl-9*H*-fluorene-2,7-diyl)bis(*N,N*-dimethylbenzenamine) **146** being obtained as a side-product of the reaction of **147** while using 4-dimethylaminobenzeneboronic

 

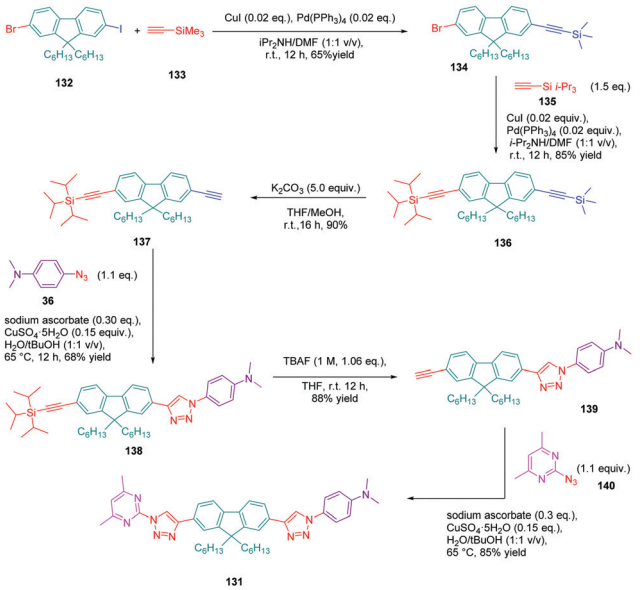

Scheme 13 Synthesis of the double triazole-bridged compound **131** starting from **132**.

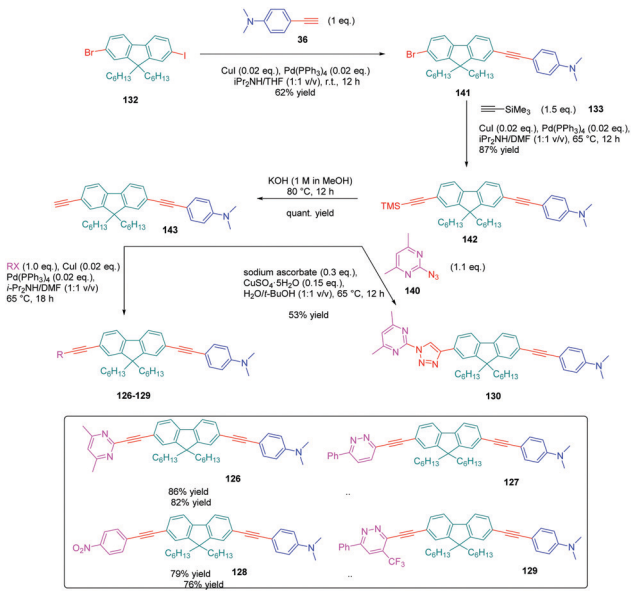

Scheme 14 Synthetic route to compounds **126–130**.

acid **148** (see Scheme 15). Surprisingly, a higher yield was obtained for the Suzuki cross coupling reaction of 3-chloro-6-phenyl-4-(trifluoromethyl)-pyridazine **149** (44% yield) than 2-iodo-4,6-dimethylpyrimidine **150** (16% yield). Generally, higher reaction yields are obtained with iodo-derivatives than chloro-derivatives due to the higher polarization of the C–I bond.[77–85] In the present case, the higher reactivity of 3-chloro-6-phenyl-4-(trifluoromethyl)pyridazine **149** was assigned to the presence of the trifluoromethyl group, activating the C–Cl bond.

The UV-visible absorption and photoluminescence properties of the different dyes were examined in dichloromethane and a summary of the photophysical properties is provided in Table 7.

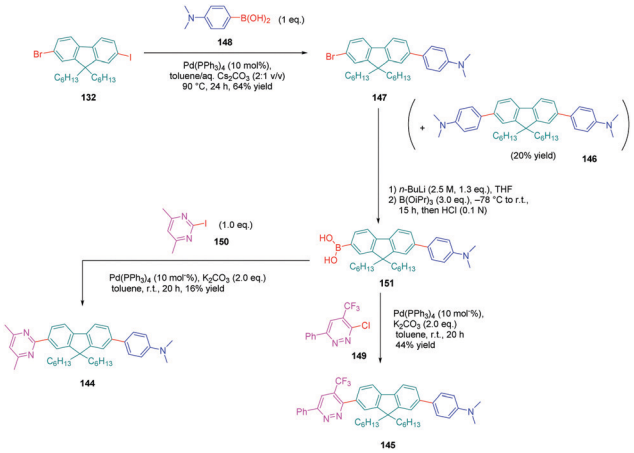

Scheme 15 Successive Suzuki cross coupling reactions enabling the formation of the push–pull derivatives **144** and **145**.

Table 7 Photophysical properties of compounds **126–131**, **144** and **145** reported in ref. 74

| Dyes | $\lambda_{abs}$ (nm) | $\lambda_{em}$ (nm) | Stokes shift ($cm^{-1}$) | $\varepsilon$ ($M^{-1}$ $cm^{-1}$) |
|---|---|---|---|---|
| **131** | 334 | 422 | 6243 | 82 000 |
| **130** | 362 | 450 | 5402 | 71 500 |
| **128** | 391 | 474 | 4478 | 51 900 |
| **129** | 392 | 500 | 5510 | 74 700 |
| **127** | 377 | 539 | 7972 | 58 100 |
| **126** | 372 | 515 | 7464 | 52 094 |
| **145** | 358 | 423 | 4292 | 39 300 |
| **144** | 360 | 483 | 7074 | 58 800 |

Considering that all dyes possess the same electron donating group but differ in the electron accepting group and the nature of the conjugated spacer, a comparison could be established.

First, all dyes exhibited an absorption maximum located in the UV-visible range. The maximum absorption was determined at 334 nm for **131** and 392 nm for **129**, which possess the most red-shifted absorption of the series. For a similar electron-donating moiety, a dramatic decrease of the PLQY was determined for **145**. Indeed, compared to **144** for which a PLQY of 0.69 was measured, this value decreased to 0.01 for **145**, this compound being almost not emissive.

This result was assigned to the presence of the $CF_3$-group inducing a torsion of the molecule and breaking the π-conjugation. The comparison between **126**, **127** and **129** and the reference compound **128** revealed an appreciable red-shift of the emission maxima upon replacing the nitrobenzene group of **128** by diazine groups. The most red-shifted emission was found for **127**, peaking at 539 nm. Introduction of the electron-withdrawing trifluoromethyl-pyridazine group in **129** did not significantly modify the absorption maximum compared to **128**. Finally, using **126**, **130**, **131** and **144** exhibiting the same electron donating and accepting groups, the influence of the linkage could be determined. Thus, while replacing a single bond by an ethynyl spacer and triazole rings, a significant enhancement of the molar extinction coefficient could be determined, peaking at 82 000 $M^{-1}$ $cm^{-1}$ for **131**. Conversely, a blue-shift of the absorption maximum was

Table 8 Two photon absorption cross-sections $\delta_{TPA}$ and wavelength of the maximum TPA cross-section reported in ref. 74

| Dyes | $\lambda_{TPA}{}^{a}$ (nm) | $\delta_{TPA}{}^{b}$ ($10^{-50}$ cm$^4$ s photon$^{-1}$) |
|---|---|---|
| **131** | 700 | 39 |
| **130** | 760 | 148 |
| **128** | 750 | 114 |
| **129** | 740 | 367 |
| **127** | 780 | 269 |
| **126** | 760 | 82 |
| **144** | 700 | 263 |
| **145** | 740 | 123 |

[a] Wavelength of the maximum TPA cross-section. [b] TPA cross-section.

found for **131** compared to **144** (334 nm *vs.* 360 nm respectively), evidencing a clear interruption of the conjugation when a 1,2,3-triazole ring is introduced as the spacer. Finally, two photon absorption (TPA) measurements were realized on these molecules and the results are summarized in Table 8. By using a femtosecond laser pulse, the solutions could be excited in the 690–940 nm region. All triazole-based dyes displayed a maximum wavelength for the TPA absorption in the near infrared region. While comparing **126**, **130** and **131**, the benefits of the presence of one triazole ring were clearly evidenced, the TPA absorption being shifted from 740 to 760 nm. Conversely and as observed for photoluminescence, the presence of two triazole rings in **131** was detrimental for the photophysical properties, a blue-shift as high as 60 nm being detected for the TPA maximum wavelength between **144** and **131**.

The pyrimidine moiety has been at the basis of numerous push–pull dyes, this group constituting a relatively good electron acceptor. Notably, a series of eight push-triazole-pull dyes **152–159** differing in the end-groups was synthesized using the click reaction. This series was achieved by click chemistry between the azidopyrimidine **140** and the different alkynes **94** and **160–166** in a mixture of water/*tert*-butanol, in the presence of copper sulfate and sodium ascorbate, producing the eight dyes **152–159** with reaction yields ranging from 58 to 99% (see Scheme 16). Here again, two structural analogues of **152** were prepared, the first one (**167**) resulting from a click reaction between 4,6 dimethyl-2-ethynylpyrimidine **168** and 4-azido-*N*,*N*-dimethylaniline **36**. Synthesis of this compound **167** was previously reported in the literature (see Scheme 16).[86,87]

The second one (**169**) was obtained by a Sonogashira cross coupling reaction of 2-iodo-4,6-dimethylpyrimidine **150** with 4-ethynylaniline **94**, providing the compound in 81% yield (see Scheme 16).

As anticipated, all dyes exhibited absorption centered in the UV region, ranging from 244 nm for **156** to 222 nm for **153**. Conversely, part of the molecules could emit in the visible range, from 476 nm for **153** and **154** to 486 nm for **152**. A major impact of the substitution pattern was demonstrated. Thus, alkylation of the amine group of **154** resulted in a red-shift of both the absorption and the emission properties of **152** and **153** due to an improved electron-donating ability. Conversely, the methoxy group is a less efficient electron donor than a dimethylamino or a diphenylamino group, which was confirmed by the

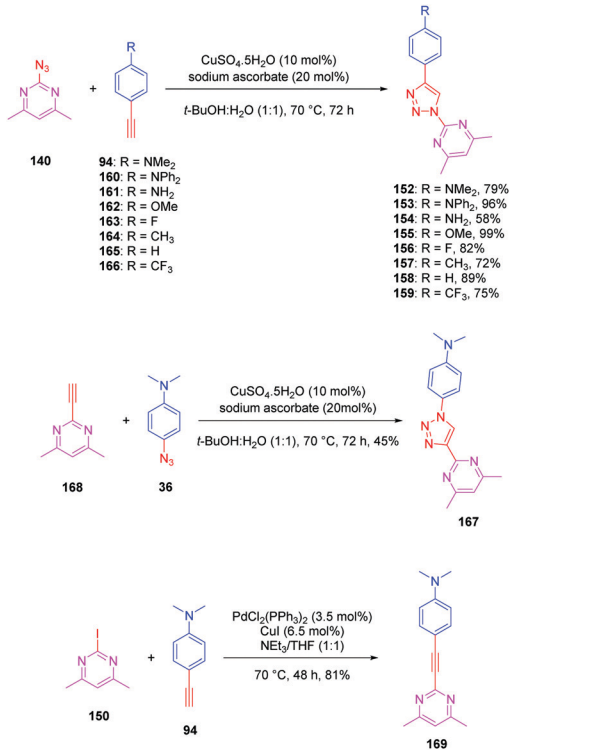


Scheme 16 Synthesis of the triazole-based series **152–159**, **167** and **169** and the corresponding reaction yields.

blue-shift of both the absorption and the emission peaks of **154** (see Table 9). While comparing **152** and **167**, inversion of the triazole ring in **167** resulted in a blue-shift of the absorption and the emission maxima, together with a decrease of the PLQY.

Table 9 Two photon absorption cross-sections $\delta_{TPA}$ and wavelength of the maximum TPA cross-section reported in ref. 85

| Dyes | $\lambda_{abs}$ (nm) | $\varepsilon$ (M$^{-1}$ cm$^{-1}$) | $\lambda_{em}$ (nm) | Stokes shift (cm$^{-1}$) | $\Phi_F{}^{a}$ |
|---|---|---|---|---|---|
| **152** | 289 | 24 386 | 486 | 14 026 | 0.47 |
| **153** | 333 | 21 427 | 476 | 9022 | 0.45 |
| **154** | 267 | 25 698 | 476 | 16 445 | 0.30 |
| **155** | 254 | 46 211 | 389 | 13 663 | 0.01 |
| **156** | 244 | 18 069 | 345 | 11 998 | $<0.01$ |
| **157** | 250 | 18 943 | 364 | 12 527 | $<0.01$ |
| **158** | 246 | 25 697 | — | — | — |
| **159** | 254 | 20 753 | — | — | — |
| **167** | 250 | 13 893 | 434 | 16 958 | 0.33 |
| **169** | 357 | 42 161 | 447 | 5640 | 0.04 |

All spectra were recorded in $CH_2Cl_2$ at 25 °C. [a] Quantum yield (±10%) of fluorescence determined by using harmane in 0.1 M $H_2SO_4$ as a standard ($\Phi_F$ = 0.83).

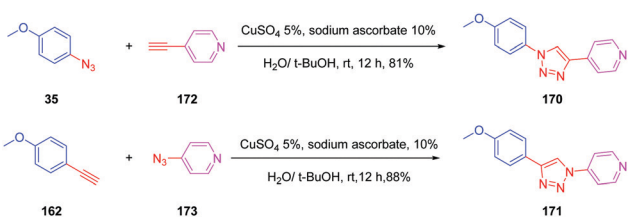


Scheme 17 Synthesis of pyridyloxazole-type fluorophores **170** and **171**.

 

On replacement of the triazole ring in **152** and **167** by an ethynyl group, a drastic red-shift of the absorption maximum occurred (357 nm *vs.* 250 nm for **167**). On the contrary, the small Stokes shift and the low PLQY of **167** confirmed the conclusions previously established from a similar comparison. To get a deeper insight into the optical properties of the different dyes, DFT calculations were carried out. For most of the compounds a fully planar structure was found except for **167**, which presented a dihedral angle of 35° between the phenyl ring and the triazole ring.

This deviation supports the blue-shift observed both in absorption and emission for **167** relative to **152**. Theoretical calculations also revealed the absorption spectrum of **169** to be dominated by two main transitions, assigned to the HOMO → LUMO and the HOMO−1 → LUMO transitions. Considering that for all triazole-based dyes a unique transition corresponding to the HOMO → LUMO transition could be theoretically determined, comparison between **169** and **152** or **167** is relatively difficult. Besides, the higher PLQY of **152** compared to **169** is indicative of better electron transfer when a triazole ring is used. Parallel to this, DFT calculations also showed the

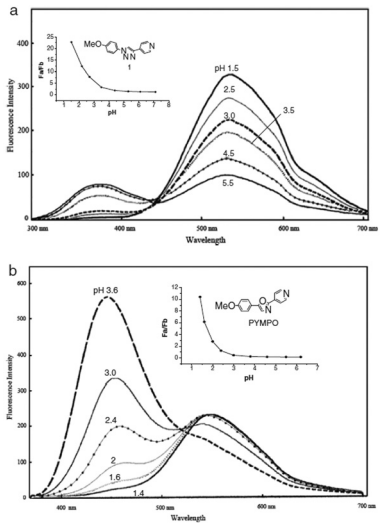


Fig. 11 Fluorescence emission spectra of PYMPO (b) and its triazole-based analogue **170** (a). Reproduced with permission from ref. 88. Copyright 2007, The Chemical Society of Japan (CSJ).

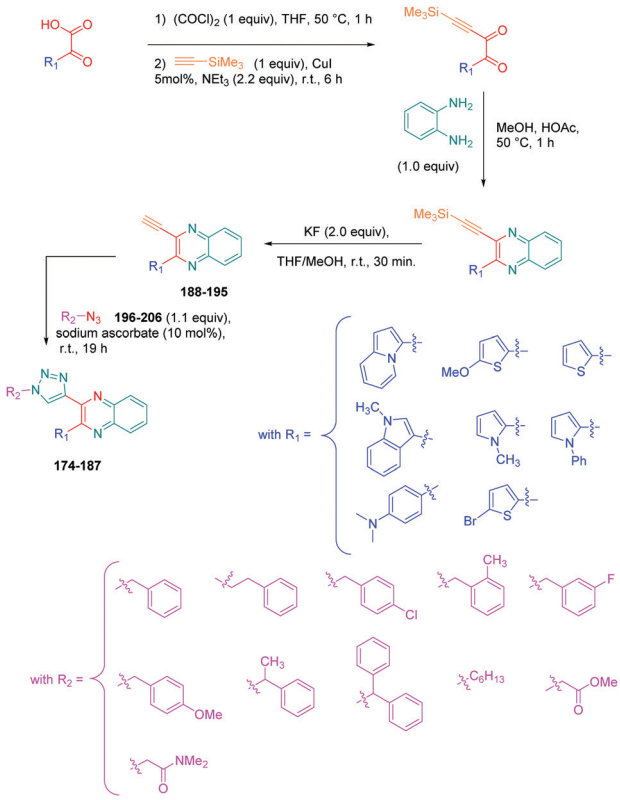


Scheme 18 One pot process for synthesis of quinoxalines **174–187**.

Table 10 Two photon absorption cross-sections $\delta_{TPA}$ and wavelength of the maximum TPA cross-section reported in ref. 91

| | $R_1$ | $R_2$ | Product | Yield | $\lambda_{max}$, abs[a] [nm] | $\lambda_{max}$, em[b] [nm] |
|---|---|---|---|---|---|---|
| **174** |  |  | 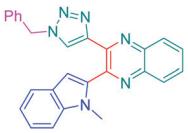 | 82 | 262 | 541 |
| **175** |  |  | 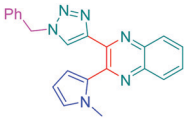 | 77 | 292 | 548 |
| **176** | 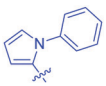 |  | 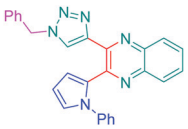 | 56 | 393 | n.d. |
| **177** |  |  | 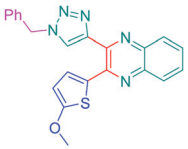 | 72 | 259 | n.d. |
| **178** |  |  | 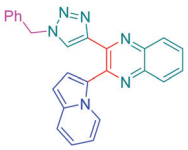 | 42 | 293 | n.d. |
| **179** | 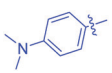 |  | 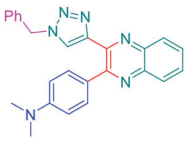 | 62 | 384 | 613 |
| **180** |  |  | 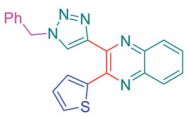 | 66 | n.d. | 440 |
| **181** |  |  | 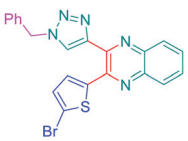 | 70 | n.d. | n.d. |

n.d.: not determined. [a] Recorded in $CH_2Cl_2$, $C = 10^{-5}$ M at $T = 293$ K. [b] Recorded in $CH_2Cl_2$.

electron density of **152** to be more separated than in **169**. Indeed, if the LUMO level of **169** extends over the phenyl ring of the donor, conversely, for **152**, the LUMO level is strictly confined on the electron accepting group. In this context, a higher electronic redistribution occurs upon excitation of **152** compared to **167**. The influence of the orientation of the phenyl ring on the optical properties was not limited to diazine-based electron acceptors. Pyridine was also selected as a candidate for carrying out a similar study.[88] The synthetic route is reported in Scheme 17 and the two dyes **170** and **171** could be obtained with reaction yields close to 90%.

Specifically, **170** and **171** were prepared for their structural analogy to PYMPO, which is a pH probe characterized by strong emission but which is difficult to prepare.[89,90] Considering that pyridine is highly sensitive to the pH of the reaction medium and can potentially be protonated under acidic conditions, and that the 1,2,3-triazole ring can be easily formed starting from easily accessible intermediates, **170** and **171** were thus considered as candidates of choice to act as a pH probe to examine biological samples *in vivo*. Examination of the PL spectra at pH below 7 revealed the fluorescence intensity of **170** to decrease while increasing the pH. No modification of the emission maxima was also detected while varying the pH. Comparison of the PL spectra of **170** and **171** revealed a major difference in the number of peaks. Thus, if two peaks could be detected in the PL spectra of **170**, a unique peak could be found for **171**, irrespective of the pH (see Fig. 11). Finally, comparison of **170** with PYMPO revealed a 25-fold enhancement of the pH-sensitivity of **170** for pH ranging from 1.5 to 7.

Luminescent molecules can also be obtained using a complex procedure as exemplified in the following series of fluorophores.[91] Fourteen 3-triazolylquinoxaline derivatives **174–188** were notably prepared using a glyoxylation–alkynylation–cyclocondensation–Cu-catalyzed alkyne–azide cycloaddition (GACC-CuAAC) sequence

Table 11 Two photon absorption cross-sections $\delta_{TPA}$ and wavelength of the maximum TPA cross-section reported in ref. 91

| | $R_1$ | $R_2$ | Product | Yield | $\lambda_{max}$, abs[a] [nm] | $\lambda_{max}$, em[b] [nm] |
|---|---|---|---|---|---|---|
| **174** |  |  | 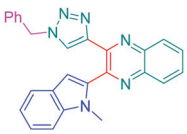 | 82 | 262<br>292<br>393 | 541 |
| **182** |  | 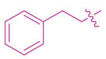 | 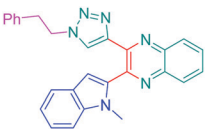 | 73 | n.d. | n.d. |
| **183** |  | 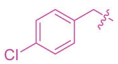 | 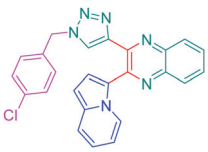 | 48 | 265<br>396 | 541 |
| **184** |  |  | 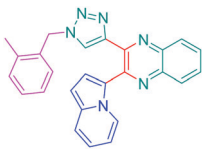 | 79 | n.d. | n.d. |
| **185** |  | 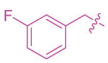 | 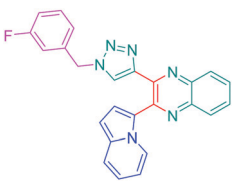 | 58 | 265<br>396 | 547 |
| **186** |  | 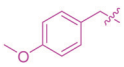 | 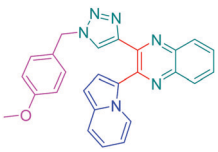 | 46 | 263<br>290<br>392 | 541 |
| **187** |  |  | 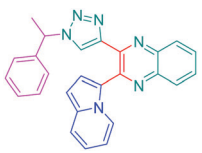 | 69 | 264<br>292<br>391 | 540 |

n.d.: not determined. [a] Recorded in $CH_2Cl_2$, $C = 10^{-5}$ M at $T = 293$ K. [b] Recorded in $CH_2Cl_2$.

 

requiring five components to proceed. In this one pot reaction, coupling glyoxylation of rich π-electron heterocycles, Castro alkynylation of acyl chlorides by alkynes, and cyclocondensation of diketones with diphenylamine followed by a click reaction of various azide derivatives **194–204** with alkynes **189–193** furnished **174–188** with reaction yields ranging from 42% for **178** to 82% for **174** (see Scheme 18). Two series of molecules can be distinguished. As shown in Table 10, the first series (**174–181**) differs from the second one by the nature of the electron donating π-heterocycles. Conversely, the second series (**182–187**) varies only in the substituents on the triazole ring, the other substituents remaining the same (see Table 11). If change of the electron donating π-heterocycles could impact the emission wavelength, modification of the pendant group introduced by means of the azide derivatives did not significantly change the photophysical properties of the second series of compounds (see Tables 10 and 11).

In fact, by improving the electron-donating ability of the heterocycle, a bathochromic shift was observed from 2-thienyl (**180**) to 1-methylpyrrolyl (**175**), 1-indolyl (**174**) and finally dimethylaminobenzene (**179**) groups. Using this strategy, a red-shift of the absorption maximum from 368 nm for **180** to 393 nm for **179** was observed. For all dyes, relatively low PLQYs were determined, and this counter-performance was assigned to an internal torsion in the ground and the excited states resulting from the presence of the triazole ring. DFT studies confirmed the lack of influence of the triazolyl substituents on the intramolecular charge transfer, since the HOMO is localized on the rich-electron heterocycle and the LUMO on the quinoxaline core. Moreover, optimization of the geometries of all dyes confirmed the rotation of the triazolyl ring, impacting the conjugation of this substituent with the rest of the molecule. This absence of an effect of the appended triazole ring on the photophysical properties could constitute an advantage for future applications of quinoxalozine compounds in materials or biological applications.

## 3. Conclusions

The discovery of click chemistry at the beginning of the 21st century has clearly reinvented the way to produce molecules. The effect of triazole on the photophysical properties has been clearly evidenced over the years. If the presence of the 1,2,3-triazole ring has clearly demonstrated a negative impact on the π-conjugation when used as a spacer in push–pull dyes, benefits of this group were also demonstrated by providing a higher Stokes shift and higher PLQYs to molecules comprising this group. Besides, by its easiness to be handled and the different studies reporting the preparation of numerous derivatives, the advantages of click chemistry to rapidly develop a wide range of derivatives have been clearly demonstrated. Considering the versatility of click chemistry, the reduction of π-conjugation in push–pull dyes compared to alkene, alkyne and other π-conjugated spacers will certainly be solved in the future. Concerning the future applications in which click-chemistry-based dyes could be involved, photopolymerization, which is a rapidly expanding research field, is one of those. Notably, photopolymerists are searching new dyes with optical properties that could be finely tuned allowing to efficiently initiate and control a polymerization process. The same exigence exists for non-linear optical applications with the design of dyes with carefully controlled absorption properties. The versatility of click chemistry will certainly allow during the next decade the design of efficient photoinitiators or NLO dyes.

## Conflicts of interest

There are no conflicts to declare.

## Acknowledgements

This research was funded by Aix-Marseille University and the Centre National de la Recherche Scientifique. The Direction Générale de l'Armement (DGA) is acknowledged for its financial support through the PhD grant of Damien Brunel.

## References

1 C. W. Tornøe, C. Christensen and M. Meldal, *J. Org. Chem.*, 2002, **67**, 3057–3064.
2 V. V. Rostovtsev, L. G. Green, V. V. Fokin and K. B. Sharpless, *Angew. Chem., Int. Ed.*, 2002, **41**, 2596–2599.
3 R. Huisgen, G. Szeimies and L. Möbius, *Chem. Ber.*, 1967, **100**, 2494–2507.
4 X. Jiang, X. Hao, L. Jing, G. Wu, D. Kang, X. Liu and P. Zhan, *Expert Opin. Drug Discovery*, 2019, **14**, 779–789.
5 P. Thirumurugan, D. Matosiuk and K. Jozwiak, *Chem. Rev.*, 2013, **113**, 4905–4979.
6 J.-P. Meyer, P. Adumeau, J. S. Lewis and B. M. Zeglis, *Bioconjugate Chem.*, 2016, **27**, 2791–2807.
7 A. Marrocchi, A. Facchetti, D. Lanari, S. Santoro and L. Vaccaro, *Chem. Sci.*, 2016, **7**, 6298–6308.
8 D. Döhler, P. Michael and W. H. Binder, *Acc. Chem. Res.*, 2017, **50**, 2610–2620.
9 K. Kacprzak, I. Skiera, M. Piasecka and Z. Paryzek, *Chem. Rev.*, 2016, **116**, 5689–5743.
10 V. K. Tiwari, B. B. Mishra, K. B. Mishra, N. Mishra, A. S. Singh and X. Chen, *Chem. Rev.*, 2016, **116**, 3086–3240.
11 A. Saeed, F. A. Larik and P. A. Channar, *Res. Chem. Intermed.*, 2016, **42**, 6805–6813.
12 N. G. Aher, V. S. Pore, N. N. Mishra, A. Kumar, P. K. Shukla, A. Sharma and M. K. Bhat, *Bioorg. Med. Chem. Lett.*, 2009, **19**, 759–763.
13 M. Meldal and C. W. Tornøe, *Chem. Rev.*, 2008, **108**, 2952–3015.
14 J. E. Moses and A. D. Moorhouse, *Chem. Soc. Rev.*, 2007, **36**, 1249–1262.
15 M. Juricek, P. H. J. Kouwer and A. E. Rowan, *Chem. Commun.*, 2011, **47**, 8740–8749.
16 P. Xiao, W. Hong, Y. Li, F. Dumur, B. Graff, J.-P. Fouassier, D. Gigmes and J. Lalevée, *Polym. Chem.*, 2014, **5**, 2293–2300.
17 P. Xiao, F. Dumur, D. Thirion, S. Fagour, A. Vacher, X. Sallenave, B. Graff, J.-P. Fouassier, D. Gigmes and J. Lalevée, *Macromolecules*, 2013, **46**, 6786–6793.

18 P. Xiao, F. Dumur, T. T. Bui, X. Sallenave, F. Goubard, B. Graff, F. Morlet-Savary, J.-P. Fouassier, D. Gigmes and J. Lalevée, *ACS Macro Lett.*, 2013, **2**, 736–740.
19 P. Xiao, F. Dumur, B. Graff, D. Gigmes, J.-P. Fouassier and J. Lalevée, *Macromolecules*, 2013, **46**, 7661–7667.
20 A. Al Mousawi, F. Dumur, J. Toufaily, T. Hamieh, B. Graff, D. Gigmes, J.-P. Fouassier and J. Lalevée, *Macromolecules*, 2017, **50**, 2747–2758.
21 J. Zhang, N. Zivic, F. Dumur, P. Xiao, B. Graff, D. Gigmes, J.-P. Fouassier and J. Lalevée, *J. Polym. Sci., Part A: Polym. Chem.*, 2015, **53**, 445–451.
22 P. Xiao, M. Frigoli, F. Dumur, B. Graff, D. Gigmes, J.-P. Fouassier and J. Lalevée, *Macromolecules*, 2014, **47**, 106–112.
23 M.-A. Tehfe, F. Dumur, B. Graff, F. Morlet-Savary, D. Gigmes, J.-P. Fouassier and J. Lalevée, *Polym. Chem.*, 2013, **4**, 3866–3875.
24 M. Parent, O. Mongin, K. Kamada, C. Katan and M. Blanchard-Desce, *Chem. Commun.*, 2005, 2029–2031.
25 P. D. Zoon, I. H. M. van Stokkum, M. Parent, O. Mongin, M. Blanchard-Desce and A. M. Brouwer, *Phys. Chem. Chem. Phys.*, 2010, **12**, 2706–2715.
26 L. Porrès, O. Mongin, C. Katan, M. Charlot, T. Pons, J. Mertz and M. Blanchard-Desce, *Org. Lett.*, 2004, **6**, 47–50.
27 M. G. Silly, L. Porrès, O. Mongin, P. A. Chollet and M. Blanchard-Desce, *Chem. Phys. Lett.*, 2003, **379**, 74–80.
28 H. Qin, S. Wenger, M. Xu, F. Gao, X. Jing, P. Wang, S. M. Zakeeruddin and M. Grätzel, *J. Am. Chem. Soc.*, 2008, **130**, 9202–9203.
29 H. Li, K. Fu, A. Hagfeldt, M. Grätzel, S. G. Mhaisalkar and A. C. Grimsdale, *Angew. Chem., Int. Ed.*, 2014, **53**, 4085–4088.
30 G. Zhang, H. Bala, Y. Cheng, D. Shi, X. Lv, Q. Yu and P. Wang, *Chem. Commun.*, 2009, 2198–2200.
31 H. Im, S. Kim, C. Park, S.-H. Jang, C.-J. Kim, K. Kim, N.-G. Park and C. Kim, *Chem. Commun.*, 2010, **46**, 1335–1337.
32 W. Zeng, Y. Cao, Y. Bai, Y. Wang, Y. Shi, M. Zhang, F. Wang, C. Pan and P. Wang, *Chem. Mater.*, 2010, **22**, 1915–1925.
33 P. Blanchard, C. Malacrida, C. Cabanetos, J. Roncali and S. Ludwigs, *Polym. Int.*, 2019, **68**, 589–606.
34 R. Rybakiewicz, M. Zagorska and A. Pron, *Chem. Pap.*, 2017, **71**, 243–268.
35 A. Cravino, S. Roquet, O. Alévêque, P. Leriche, P. Frère and J. Roncali, *Chem. Mater.*, 2006, **18**, 2584–2590.
36 M. Bourass, A. T. Benjelloun, M. Benzakour, M. Mcharfi, F. Jhilal, M. Hamidiband and M. Bouachrine, *New J. Chem.*, 2017, **41**, 13336–13346.
37 T. Duan, K. Fan, Y. Fu, C. Zhong, X. Chen, T. Peng and J. Qin, *Dyes Pigm.*, 2012, **94**, 28–33.
38 S. Wen, J. Pei, Y. Zhou, P. Li, L. Xue, Y. Li, B. Xu and W. Tian, *Macromolecules*, 2009, **42**, 4977–4984.
39 K. Sharma, V. Sharma and S. S. Sharma, *Nanoscale Res. Lett.*, 2018, **13**, 381.
40 F. Lenzmann, J. Krueger, S. Burnside, K. Brooks, M. Grätzel, D. Gal, S. Rühle and D. Cahen, *J. Phys. Chem. B*, 2001, **105**, 6347–6352.
41 P. Kautny, D. Bader, B. Stöger, G. A. Reider, J. Fröhlich and D. Lumpi, *Chem. – Eur. J.*, 2016, **22**, 18887–18898.
42 C. Katan, P. Savel, B. M. Wong, T. Roisnel, V. Dorcet, J. L. Fillaut and D. Jacquemin, *Phys. Chem. Chem. Phys.*, 2014, **16**, 9064–9073.
43 N. Mataga, Y. Kaifu and M. Koizumi, *Bull. Chem. Soc. Jpn.*, 1956, **29**, 465–470.
44 J. L. Oudar and D. S. Chemla, *J. Chem. Phys.*, 1977, **66**, 2664–2668.
45 S. Gronowitz and T. Frejd, *Chem. Heterocycl. Compd.*, 1978, **14**, 353–367.
46 B. Iddon, *Heterocycles*, 1983, **20**, 1127–1171.
47 T. L. Gilchrist, *Adv. Heterocycl. Chem.*, 1987, **41**, 41–74.
48 D. Lumpi, E. Horkel, B. Stoeger, C. Hametner, F. Kubel, G. A. Reider and J. Froehlich, *Proc. SPIE*, 2011, **8306**, 830615/1.
49 D. Lumpi, F. Glöcklhofer, B. Holzer, B. Stöger, C. Hametner, G. A. Reider and J. Fröhlich, *Cryst. Growth Des.*, 2014, **14**, 1018–1031.
50 D. Lumpi, J. Steindl, S. Steiner, V. Carl, P. Kautny, M. Schön, F. Glöcklhofer, B. Holzer, B. Stöger, E. Horkel, C. Hametner, G. Reider, M. D. Mihovilovic and J. Fröhlich, *Tetrahedron*, 2017, **73**, 472–480.
51 P. D. Jarowski, Y.-L. Wu, W. B. Schweizer and F. Diederich, *Org. Lett.*, 2008, **10**, 3347–3350.
52 K. Staub, G. A. Levina, S. Barlow, T. C. Kowalczyk, L. S. Lackritz, M. Barzoukas, A. Fort and S. R. Marder, *J. Mater. Chem.*, 2003, **13**, 825–833.
53 T. Michinobu, J. C. May, J. H. Lim, C. Boudon, J. P. Gisselbrecht, P. Seiler, M. Gross, I. Biaggio and F. Diederich, *Chem. Commun.*, 2005, 737–739.
54 B. B. Frank, P. R. Laporta, B. Breiten, M. C. Kuzyk, P. D. Jarowski, W. B. Schweizer, P. Seiler, I. Biaggio, C. Boudon, J.-P. Gisselbrecht and F. Diederich, *Eur. J. Org. Chem.*, 2011, 4307–4317.
55 D. J. V. C. van Steenis, O. R. P. David, G. F. P. van Strijdonck, J. H. van Maarseveen and J. N. H. Reek, *Chem. Commun.*, 2005, 4333–4335.
56 Y. Zhu, S. Guang, X. Su, H. Xu and D. Xu, *Dyes Pigm.*, 2013, **97**, 175–183.
57 G. Kremser, O. T. Hofmann and S. Sax, *Monatsh. Chem.*, 2008, **139**, 223–231.
58 Y. L. Liu, J. K. Feng and A. M. Ren, *J. Phys. Chem. A*, 2008, **112**, 3157–3164.
59 S. S. Bag and R. Kundu, *J. Org. Chem.*, 2011, **76**, 3348–3356.
60 K. E. Beatty, J. C. Liu, F. Xie, D. C. Dieterich, E. M. Schuman, Q. Wang and D. A. Tirrell, *Angew. Chem., Int. Ed.*, 2006, **45**, 7364–7367.
61 K. E. Beatty, F. Xie, Q. Wang and D. A. Tirrell, *J. Am. Chem. Soc.*, 2005, **127**, 14150–14151.
62 M. Sawa, T.-L. Hsu, T. Itoh, M. Sugiyama, S. R. Hanson, P. K. Vogt and C.-H. Wong, *Proc. Natl. Acad. Sci. U. S. A.*, 2006, **103**, 12371–12376.
63 Q. Wang, T. R. Chan, R. Hilgraf, V. V. Fokin, K. B. Sharpless and M. G. Finn, *J. Am. Chem. Soc.*, 2003, **125**, 3192–3193.
64 Z. Zhou and C. J. Fahrni, *J. Am. Chem. Soc.*, 2004, **126**, 8862–8863.
65 F. Xie, K. Sivakumar, Q. Zeng, M. A. Bruckman, B. Hodges and Q. Wang, *Tetrahedron*, 2008, **64**, 2906–2914.
66 D. Li, S. Wang, Z. Lei, C. Sun, A. M. El-Toni, M. S. Alhoshan, Y. Fan and F. Zhang, *Anal. Chem.*, 2019, **91**, 4771–4779.

 

67 F. Ding, C. Li, Y. Xu, J. Li, H. Li, G. Yang and Y. Sun, *Adv. Healthcare Mater.*, 2018, **7**, 1800973.
68 R. Zhang, Y. Xu, Y. Zhang, H. S. Kim, A. Sharma, J. Gao, G. Yang, J. S. Kim and Y. Sun, *Chem. Sci.*, 2019, **10**, 8348–8353.
69 L. Tua, Y. Xu, Q. Ouyang, X. Li and Y. Sun, *Chin. Chem. Lett.*, 2019, **30**, 1731–1737.
70 F. Ding, Y. Fan, Y. Sun and F. Zhang, *Adv. Healthcare Mater.*, 2019, **8**, 1900260.
71 F. Ding, Z. Chen, W. Y. Kim, A. Sharma, C. Li, Q. Ouyang, H. Zhu, G. Yang, Y. Sun and J. S. Kim, *Chem. Sci.*, 2019, **10**, 7023–7028.
72 Y. Xu, M. Tian, H. Zhang, Y. Xiao, X. Hong and Y. Sun, *Chin. Chem. Lett.*, 2018, **29**, 1093–1097.
73 J. Li, M. Hu and S. Q. Yao, *Org. Lett.*, 2009, **11**, 3008–3011.
74 C. Denneval, O. Moldovan, C. Baudequin, S. Achelle, P. Baldeck, N. Plé, M. Darabantu and Y. Ramondenc, *Eur. J. Org. Chem.*, 2013, 5591–5602.
75 S. Achelle, N. Plé and A. Turck, *RSC Adv.*, 2011, **1**, 364–388.
76 S. Achelle and N. Plé, *Org. Synth.*, 2012, **9**, 163–187.
77 A. F. Littke and G. C. Fu, *Angew. Chem., Int. Ed.*, 2002, **41**, 4176–4211.
78 B. U. W. Maes, P. Tapolcsányi, C. Meyers and P. Mátyus, *Curr. Org. Chem.*, 2006, **10**, 377–417.
79 S. Nara, J. Martinez, C. G. Wermuth and I. Parrot, *Synlett*, 2006, 3185–3204.
80 A. Turck, N. Plé, L. Mojovic and G. Queguiner, *Bull. Soc. Chim. Fr.*, 1993, **130**, 488–492.
81 S. Achelle, N. Plé, A. Turck, J. P. Bouillon and C. Portella, *J. Heterocycl. Chem.*, 2006, **43**, 1243–1249.
82 S. Achelle, Y. Ramondenc, F. Marsais and N. Plé, *Eur. J. Org. Chem.*, 2008, 3129–3140.
83 S. Tumkevicius, J. Donkova, I. Baskirova and A. Voitechovicius, *J. Heterocycl. Chem.*, 2009, **46**, 960–964.
84 S. Asano, S. Kamioka and Y. Isobe, *Tetrahedron*, 2012, **68**, 272–279.
85 A. S. Cornec, C. Baudequin, C. Fiol-Petit, N. Plé, G. Dupas and Y. Ramondenc, *Eur. J. Org. Chem.*, 2013, 1908–1915.
86 K. D. Grimes, A. Gupte and C. C. Aldrich, *Synthesis*, 2010, 1441–1448.
87 T. Sakamoto, M. Shiraiwa, Y. Kondo and H. Yamanaka, *Synthesis*, 1983, 312–314.
88 J. Shi, L. Liu, J. He, X. Meng and Q. Guo, *Chem. Lett.*, 2007, **36**, 1142–1143.
89 S. Charier, O. Ruel, J.-B. Baudin, D. Alcor, J.-F. Allemand, A. Meglio and J. Jullien, *Angew. Chem., Int. Ed.*, 2004, **43**, 4785.
90 S. Charier, O. Ruel, J.-B. Baudin, D. Alcor, J.-F. Allemand, A. Meglio, L. Jullien and B. Valeur, *Chem. – Eur. J.*, 2006, **12**, 1097–1113.
91 F. K. Merkt, K. Pieper, M. Klopotowski, C. Janiak and T. J. J. Müller, *Chem. – Eur. J.*, 2019, **25**, 9447–9455.